

Pseudogaps, Jahn-Teller distortions, and magnetic order in manganite perovskites

D. J. Singh

Complex Systems Theory Branch, Naval Research Laboratory, Washington, DC 20375-5320

W. E. Pickett

Complex Systems Theory Branch, Naval Research Laboratory, Washington, DC 20375-5320

and Department of Physics, University of California, Davis, California 95616

(Received 5 August 1997)

Local spin-density calculations are used to investigate the relationship between lattice distortions, magnetic ordering, and electronic properties in manganite perovskites. Lattice distortions are found to open pseudogaps at the middle of the majority spin e_g manifold, which are more directly related to rotations than Jahn-Teller distortion. Because the pseudogap is narrow, its effect on transport is strongly dependent on doping, falling off due to Fermi-level motion as La is replaced by divalent ions in LaMnO_3 . Structural relaxations provide evidence that unlike pure LaMnO_3 , lattice distortions in the ferromagnetically-ordered colossal-magnetoresistance (CMR) regime are relatively weakly coupled to electronic properties. These results are discussed in relation to the CMR effect. [S0163-1829(98)06401-7]

I. INTRODUCTION

The discovery of colossal magnetoresistance (CMR) in ferromagnetic (FM) manganites^{1,2} has renewed interest in these materials. One of the key outstanding problems is understanding the nature of the metal-insulator transition at the Curie temperature, T_C . As was recognized early on,³⁻⁵ strong couplings between doping level, lattice distortions, magnetic order, and electronic properties are present. LaMnO_3 occurs in strongly distorted $Pnma$ orthorhombic or closely related structures^{3,6} and is A -type antiferromagnetic (AFM) and insulating. The lattice distortions, relative to cubic perovskite, are rotations of the O octahedra and Jahn-Teller (JT) distortions that change the Mn-O bond lengths (from 1.97 Å, to 1.91, 1.96, and 2.18 Å). Here we use the term JT loosely for the component that is not rotational. The distortions may be understood qualitatively in terms of ion size and electron counting arguments: La^{3+} and Mn^{3+} ionic radii yield a large misfit parameter, $\sqrt{2}(R_O + R_{\text{Mn}})/(R_O + R_{\text{La}})$, strongly favoring rotational instabilities, while the high spin Mn^{3+} ion has a half occupied majority spin e_g orbital favoring a JT distortion. As LaMnO_3 is hole doped by substituting La^{3+} with divalent cations, the order becomes FM and lattice distortions change to more purely rotational in character.^{3,7,8} It is in this regime that CMR is observed. Several experimental and theoretical studies have suggested that lattice effects may be important in understanding the CMR effect,⁷⁻¹² but, while it is clear that there are lattice anomalies at the FM T_C , the extent to which they directly influence transport is still not established. Further, a CMR-like effect has been discovered in the related pyrochlore, $\text{Tl}_2\text{Mn}_2\text{O}_7$, which has neither lattice distortions nor the non-integral valence needed for a double exchange¹³ picture.¹⁴⁻¹⁶

Local spin-density approximation (LSDA) studies have been performed for the end-point compounds and some alloy compositions.¹⁷⁻²⁵ Besides verifying that known properties of these materials are reproduced, they have elucidated a number of aspects of the electronic and magnetic structure.

Substantially hybridized bands derived from majority spin Mn e_g states and O p states dominate the electronic structure near the Fermi energy, E_F in the metallic FM materials, while the minority spin channel is effectively insulating leading to half metallic properties.²⁴ This combined with the local moment behavior may be compatible with high resistivities in the spin-disordered state above T_C even before consideration of lattice effects. The calculations also show strong couplings between lattice distortions, magnetic order, and electronic properties at least in undoped LaMnO_3 . In particular, it is found that without lattice distortions LaMnO_3 would have a FM metallic ground state, and even if forced to be A -type AFM, it would still be metallic.²¹ Mryasov and co-workers²⁵ have also reported strong coupling between lattice distortions and exchange coupling in LaMnO_3 . With the lattice distortion, the ground state becomes A -type AFM, and is found insulating in agreement with experiment. The present paper reports further calculations aimed at better understanding the role of lattice distortions in the CMR alloys $\text{La}_{1-x}\text{D}_x\text{MnO}_3$ near $x=1/3$.

II. APPROACH

The present work used the general potential linear augmented plane-wave (LAPW) method²⁶ as in our previous studies of these manganites.²¹ Calculations were done for 20 atom $Pnma$ and 5 atom perovskite unit cells using well converged basis sets and Brillouin-zone samplings. Structural relaxations used the calculated atomic forces. Although anomalies in lattice parameters are known near T_C ,^{10,11} the lattice parameters were held fixed in the relaxations. The effect of the homogeneous strains produced by anomalies of the size measured experimentally would be small compared to the bond length and bond angle changes due to the JT and rotational distortions.²⁷

As mentioned, previous calculations have shown that undistorted A -type AFM LaMnO_3 is unstable against distortion, and that the distortion changes the electronic structure

TABLE I. Relaxed structure of FM $Pnma$ LaMnO_3 with a pseudocubic lattice parameter of 3.936 Å.

	x	y	z
La	0.535	0.250	0.007
Mn	0.000	0.000	0.000
O(1)	0.013	0.750	0.071
O(2)	0.283	0.038	0.219

from metallic to insulating. This distortion has both a strong JT component and a rotation that changes the Mn-O-Mn bond angles from 180° to $\approx 160^\circ$. However, the CMR compositions are FM, and the question of the extent to which lattice distortion affects the electronic properties remains. In order to address this, a structural relaxation was performed for LaMnO_3 within the 20 atom $Pnma$ unit cell, enforcing FM ordering, and the electronic properties compared with those of an isovolume cubic perovskite cell with FM order.

The $x = 1/3$ composition range was addressed using virtual crystal approximation calculations for $\text{La}_{2/3}\text{Ba}_{1/3}\text{MnO}_3$. Separate relaxations were performed for FM and AFM orderings, and additionally a calculation was done for a structure approximating that of $\text{La}_{0.65}\text{Ca}_{0.35}\text{MnO}_3$ as determined by Dai *et al.*⁷ These virtual-crystal calculations were done with pseudocubic lattice parameters corresponding to the volume measured by Dai *et al.*⁷ and an average A -site cation charge $Z_{\text{VC}} = 56\frac{2}{3}$. The calculated electronic structure near and below E_F should be representative of Sr or Ca substitution of La as well, since these are isovalent with Ba and the A -site cations are fully ionized. However, since Ba^{2+} ions are considerably larger than Ca^{2+} the lattice will be under compressive strain which may alter the magnitude of lattice distortions in the relaxations. The virtual-crystal approach allows self-consistent treatment of the change in charge density and carrier density. Scattering due to the random occupation of the A -site is not included. This has little effect on the broadbands characteristic of the FM majority-spin channel, but localizes the minority-spin carriers so that they cannot directly participate in transport.²⁴ In the present calculations, we find that lattice distortions bring the minority-spin band edge closer to E_F , further increasing the tendency towards minority-spin localization, and as such transport is discussed in terms of the majority-spin carriers only.

III. FERROMAGNETIC LaMnO_3

As mentioned, FM LaMnO_3 was relaxed within a pseudocubic $Pnma$ symmetry unit cell at the experimental volume of AFM LaMnO_3 . Like the AFM compound, a large rotational instability is found resulting in Mn-O-Mn bond angles of 165° . However, the final relaxed structure has almost no JT component. The relaxed crystal structure within the $\sqrt{2} \times 2 \times \sqrt{2}$ $Pnma$ cell is given in Table I. The Mn-O distances are all between 2.00 and 2.01 Å. The JT distortion occurs for AFM order but not for FM order. This provides one more indication of large magnetostructural coupling in LaMnO_3 ; other evidence is the quite different crystal structures of FM and AFM modifications of LaMnO_3 ,⁶ LSDA calculations showing that the magnetic order changes from FM to A -type AFM as the lattice is distorted from cubic to

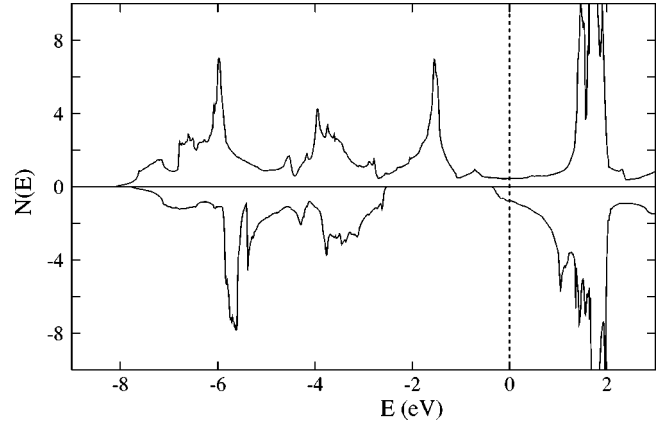


FIG. 1. Density of states of FM LaMnO_3 in the cubic perovskite structure. The majority spin is shown as positive and the minority spin as negative. $E_F = 0$.

its actual $Pnma$ structure,²¹ and the fact that the structure changes from strongly orthorhombic in LaMnO_3 to more nearly cubic around the AFM to FM transition when doped with divalent A -site cations.³

The electronic density of states (DOS) of undistorted cubic perovskite LaMnO_3 with FM order is shown in Fig. 1. The main features of the DOS have been discussed elsewhere,^{17-19,21} and are not repeated here. The spin magnetization is $3.61 \mu_B$ per formula unit. The majority-spin and minority-spin DOS at E_F , $N(E_F)$ are comparable, and conduction in both spin channels is expected. However, since we are interested in the CMR materials, where the minority carriers are localized, we discuss only the majority-spin channel. The calculations in the perovskite structure yield $N_{\uparrow}(E_F) = 0.45 \text{ eV}^{-1}$ and majority-spin Fermi velocity, $v_{F\uparrow} = 4.2 \times 10^7 \text{ cm/s}$. In Fig. 2, we show the DOS of FM LaMnO_3 in the relaxed structure. New gaps are opened between the hybridized t_{2g} and e_g manifolds in both the majority and minority channels, reflecting band narrowing due to less favorable hopping when the Mn-O-Mn bonds are bent. The distortion empties the minority states and thereby increases the magnetization to $4.00 \mu_B$ and lowers the energy

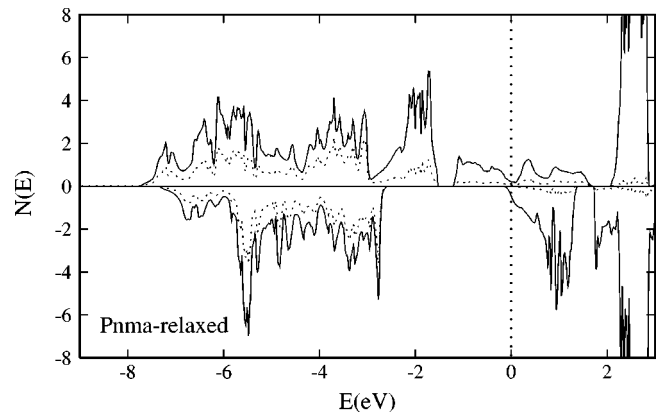


FIG. 2. Density of states of FM LaMnO_3 in the relaxed $Pnma$ structure. The dotted line is the O contribution as defined by the weight inside the O LAPW spheres. The DOS is on a per formula unit basis.

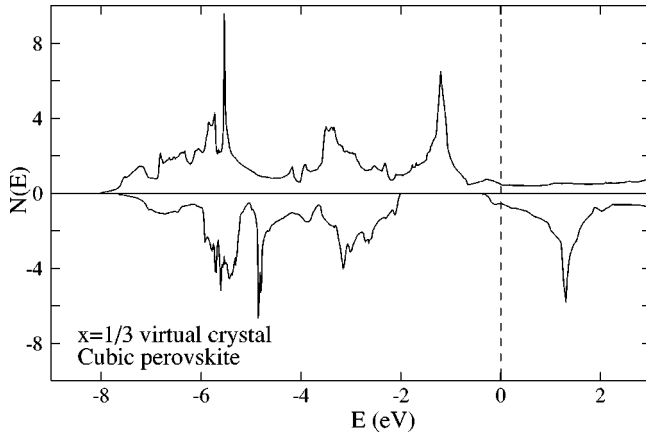


FIG. 3. Density of states for virtual crystal $(\text{La}_{2/3}\text{Ba}_{1/3})\text{MnO}_3$ in the cubic perovskite structure.

by 0.24 eV, both on a per formula unit basis. Besides making FM LaMnO_3 essentially half metallic, the distortion strongly reduces the majority-spin conductivity. $N_{\uparrow}(E_F)$ becomes 0.21 eV^{-1} , while $v_{F\uparrow x} = 2.2 \times 10^7 \text{ cm/s}$ (although the symmetry is orthorhombic there is very little anisotropy in $v_{F\uparrow}$). If changes in scattering rate due to the distortion are neglected, as may be reasonable, an eightfold reduction in majority-spin conductivity, σ due to the lattice distortion results within kinetic transport theory,²⁸ where $\sigma \propto N(E_F)v_F^2$. This strong suppression of the conductivity with the lattice distortion is due to a pseudogap that opens in the majority channel at E_F . This occurs at the center of the roughly 3 eV wide e_g (hybridized with O $p\sigma$) derived manifold.

IV. CMR REGIME: $x=1/3$

The DOS for virtual crystal $(\text{La}_{2/3}\text{Ba}_{1/3})\text{MnO}_3$ with the undistorted cubic perovskite structure is shown in Fig. 3. As mentioned, the calculation was done with a volume corresponding to that of CMR $(\text{La,Ca})\text{MnO}_3$ at $x=1/3$. The spin magnetization is $3.40\mu_B$, with majority spin $N_{\uparrow}(E_F) = 0.53 \text{ eV}^{-1}$ and $v_{F\uparrow x} = 4.2 \times 10^7 \text{ cm/s}$. These values are similar to those obtained for perovskite structure FM LaMnO_3 .

Structural relaxations were performed for the $x=1/3$ virtual crystal with both FM and A -type AFM order. The relaxed FM structure has the lower energy, by 0.014 eV/Mn, as expected. In neither case was a JT component to the distortion found. Rather, the relaxations consisted solely of small rigid rotations of the O octahedra. With FM order, the average Mn-O-Mn bond angle was 176° , while in the A -type AFM case 177° was found. These rotations are much smaller than experiment, reflecting the large Ba^{+2} ion relative to Ca^{+2} . Nonetheless, the dependence of the rotation angle on the magnetic order does indicate some magnetostructural coupling, though much weaker than in LaMnO_3 .

Dai *et al.*⁷ reported neutron refinements of lattice parameters and some bond lengths and angles for FM $Pnma$ $\text{La}_{0.65}\text{Ca}_{0.35}\text{MnO}_3$ at 300 and 40 K. The lattice parameters are very nearly pseudocubic (to about 0.2%), and the Mn-O bond lengths are all equal (to within 0.004 Å) showing a rotational component but no JT component to the distortion. The Mn-O-Mn bond angles are $160^\circ \pm 1^\circ$. We performed virtual-crystal calculations using a $Pnma$ structure derived

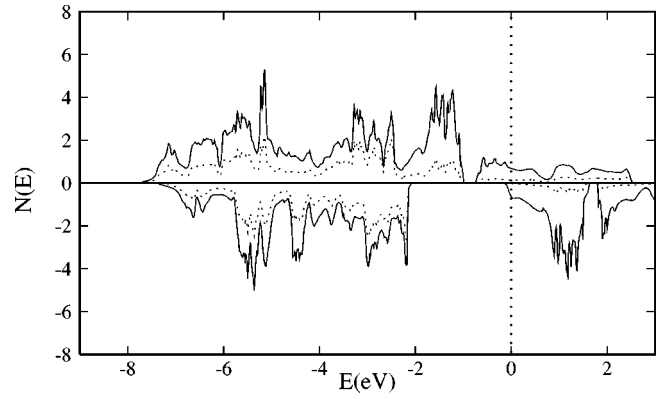


FIG. 4. Density of states of virtual crystal $(\text{La}_{2/3}\text{Ba}_{1/3})\text{MnO}_3$ in the $Pnma$ structure (see text). Note the shift of the Fermi level in the majority bands compared to Fig. 2.

from this one by making all bond lengths and Mn-O-Mn bond angles equal. The DOS is shown in Fig. 4. As in FM LaMnO_3 the distortion brings the minority-spin band edge closer to E_F . The spin magnetization increases to $3.56\mu_B$. Also like undoped LaMnO_3 , a pseudogap opens at the center of the majority-spin e_g manifold. However, at $x=1/3$, the majority e_g manifold is far from half occupied, so that this pseudogap is not near E_F . Rather, $N_{\uparrow}(E_F) = 0.68 \text{ eV}^{-1}$, which is somewhat larger than for the unrelaxed cubic perovskite structure. The velocity, $v_{F\uparrow x} = 3.1 \times 10^7 \text{ cm/s}$, is nearly isotropic and is reduced relative to the cubic structure. The net result is that the distorted structure has a value $N_{\uparrow}(E_F)v_{F\uparrow x}^2$ that is reduced to 70% of its undistorted value, indicating a relatively small effect from lattice distortions on the conductivity, particularly considering the large distortion that occurs.

V. SUMMARY AND CONCLUSIONS

LSDA calculations have shown the presence of coupling of lattice distortions and magnetic order to electronic properties in CMR alloys near $x=1/3$. However, these couplings are weak, compared to those found in pure LaMnO_3 . This is due to the narrowness of the e_g pseudogap that opens as the octahedra rotate in these materials. The calculations address the effects of static lattice distortions in fully ordered FM phases. They imply that the electron lattice coupling decreases strongly as LaMnO_3 is hole doped, a trend that is consistent with the high conductivities observed in some samples at low temperature. On the other hand, they do not address the metal-insulator transition at T_C , which occurs simultaneously with a change in magnetic order. The observations of anomalies in Debye-Waller factors and lattice parameters near T_C imply significant coupling to the lattice. It has been observed by several authors that the properties above T_C are consistent with a polaronic state with strong charge-carrier lattice interactions. Combined with the present results it would seem then that electron lattice interactions are stronger in the spin-disordered paramagnetic state than the FM state. Previous calculations have shown that these

local moment alloys are effectively half metallic when ordered and it is conjectured that this character persists locally for disordered states (strong Hund's rule). Thus carriers on Mn ions whose moments are rotated with respect to neighboring Mn will be substantially localized and will be less strongly hybridized with O, as hopping to neighbors is suppressed. These carriers occupy the JT active e_g orbital. This could lead to a local JT distortion, providing a mechanism for strongly enhanced electron lattice interaction as spin disorder increases. This picture, which is related to that of Mil-

lis and co-workers,⁹ is consistent with a good metallic ground state, rapid onset of resistivity at T_C and a highly resistive paramagnetic state.

ACKNOWLEDGMENTS

We acknowledge helpful discussions with M. Rubinstein, W. H. Butler, and J. Zhang. Work at NRL is supported by ONR. Computations were performed with the DoD HPCMO facilities at NAVO and ASC.

-
- ¹R. von Helmolt, J. Wecker, B. Holzapfel, I. Schultz, and K. Samwer, *Phys. Rev. Lett.* **71**, 2331 (1993).
- ²S. Jin, H. M. O'Bryan, T. H. Tiefel, M. McCormack, R. A. Fastnacht, R. Ramesh, and L. H. Chen, *Science* **264**, 413 (1994).
- ³E. O. Wollan and W. C. Koehler, *Phys. Rev.* **100**, 545 (1955).
- ⁴G. H. Jonker and J. H. van Santen, *Physica (Amsterdam)* **16**, 337 (1950); J. H. van Santen and G. H. Jonker, *ibid.* **16**, 599 (1950).
- ⁵C. W. Searle and S. T. Wang, *Can. J. Phys.* **48**, 2023 (1970).
- ⁶Q. Huang, A. Santoro, J. W. Lynn, R. W. Erwin, J. A. Borchers, J. L. Peng, and R. L. Greene, *Phys. Rev. B* **55**, 14 987 (1997).
- ⁷P. Dai, J. Zhang, H. A. Mook, S. H. Liou, P. A. Dowben, and E. W. Plummer, *Phys. Rev. B* **54**, R3694 (1996).
- ⁸P. G. Radaelli, D. E. Cox, M. Marezio, S. W. Cheong, P. E. Schiffer, and A. P. Ramirez, *Phys. Rev. Lett.* **75**, 4488 (1995).
- ⁹A. J. Millis, P. B. Littlewood, and B. I. Shraiman, *Phys. Rev. Lett.* **74**, 5144 (1995).
- ¹⁰M. R. Ibarra, P. A. Algarabel, C. Marquina, J. Blasco, and J. Garcia, *Phys. Rev. Lett.* **75**, 3541 (1995).
- ¹¹J. M. De Teresa, M. R. Ibarra, P. A. Algarabel, C. Ritter, C. Marquina, J. Blasco, J. Garcia, A. del Moral, and Z. Arnold, *Nature (London)* **386**, 256 (1997).
- ¹²A. P. Ramirez, P. Schiffer, S. W. Cheong, C. H. Chen, W. Bao, T. M. Palstra, P. L. Gammel, D. J. Bishop, and B. Zegarski, *Phys. Rev. Lett.* **76**, 3188 (1996).
- ¹³C. Zener, *Phys. Rev.* **82**, 403 (1951).
- ¹⁴Y. Shimakawa, Y. Kubo, and T. Manako, *Nature (London)* **379**, 53 (1996).
- ¹⁵M. A. Subramanian, B. H. Toby, A. P. Ramirez, W. J. Marshall, A. W. Sleight, and G. H. Kwei, *Science* **273**, 81 (1996).
- ¹⁶D. J. Singh, *Phys. Rev. B* **55**, 313 (1997).
- ¹⁷D. D. Sarma, N. Shanthi, S. R. Barman, N. Hamada, H. Sawada, and K. Terakura, *Phys. Rev. Lett.* **75**, 1126 (1995).
- ¹⁸I. Solovyev, N. Hamada, and K. Terakura, *Phys. Rev. Lett.* **76**, 4825 (1996).
- ¹⁹S. Satpathy, Z. S. Popovic, and F. R. Vukajlovic, *Phys. Rev. Lett.* **76**, 960 (1996).
- ²⁰W. H. Butler, X.-G. Zhang, and J. M. MacLaren, in *Magnetic Ultrathin Films and Multilayers and Surfaces*, edited by E. E. Marinero *et al.*, MRS Symposia Proceedings No. 384, (Materials Research Society, Pittsburgh, 1995), 439–443.
- ²¹W. E. Pickett and D. J. Singh, *Phys. Rev. B* **53**, 1146 (1996).
- ²²W. E. Pickett and D. J. Singh, *J. Vac. Sci. Technol. B* **14**, 3136 (1996).
- ²³W. E. Pickett and D. J. Singh, *Europhys. Lett.* **32**, 759 (1995).
- ²⁴W. E. Pickett and D. J. Singh, *Phys. Rev. B* **55**, R8642 (1997).
- ²⁵O. N. Mryasov, R. F. Sabiryanov, A. J. Freeman, and S. S. Jaswal (unpublished).
- ²⁶D. J. Singh, *Planewaves Pseudopotentials and the LAPW method* (Kluwer, Boston, 1994).
- ²⁷The changes in lattice parameters for CMR compositions around T_C are much less even than the changes due thermal expansion over temperature ranges well below T_C (Refs. 7 and 10), while the recently reported (Ref. 6) FM modifications of LaMnO_3 have homogeneous strains of less than 1% relative to cubic. Larger effects are observed near $x = 1/2$ (Ref. 8).
- ²⁸J. M. Ziman, *Principles of the Theory of Solids* (Cambridge University Press, Cambridge, 1972), and references therein.